Journal of Archaeological Science 153 (2023) 105776

Contents lists available at ScienceDirect

Journal of Archaeological Science

journal homepage: www.elsevier.com/locate/jas

Enamel thickness per masticatory phases (ETMP): A new approach to assess the relationship between macrowear and enamel thickness in the human lower first molar

Gregorio Oxilia [a,*], Mattia Zaniboni [a], Eugenio Bortolini [a,b], Jessica C. Menghi Sartorio [a], Federico Bernardini [c,d], Claudio Tuniz [d,e], Giovanni Di Domenico [f], Dinko Tresić Pavičić [g], Dženi Los [g], Siniša Radović [h], Jacqueline Balen [i], Ivor Janković [j,k], Mario Novak [j], Stefano Benazzi [a]

[a] Department of Cultural Heritage University of Bologna, Ravenna, Italy
[b] Archaeology and Human Ecology (HUMANE), IMF, CSIC, Barcelona, Spain
[c] Department of Humanistic Studies, Università Ca' Foscari, Venezia, Italy
[d] Multidisciplinary Laboratory, The Abdus Salam International Centre for Theoretical Physics, Trieste, Italy
[e] Centre for Archaeological Science, University of Wollongong, Wollongong, New South Wales, Australia
[f] Department of Physics and Earth Sciences, University of Ferrara, Ferrara, Italy
[g] Kaducej Ltd., Split, Croatia
[h] Institute for Quaternary Palaeontology and Geology, Croatian Academy of Sciences and Arts, Zagreb, Croatia
[i] Archaeological Museum in Zagreb, Croatia
[j] Centre for Applied Bioanthropology, Institute for Anthropological Research, Zagreb, Croatia
[k] Department of Anthropology, University of Wyoming, Laramie, USA

A R T I C L E I N F O

Keywords:
Bronze age
Permanent first molar
Enamel Thickness
Non-invasive approach
Virtual anthropology
Croatia
Dental wear pattern

A B S T R A C T

Many anthropological studies have examined the functional implications of enamel thickness in human dental crowns. Despite limitations, Enamel thickness (ET) values are still used to infer taxonomic attribution in the genus *Homo*, and to identify mechanisms of functional adaptation against macrowear. However, only a few studies have tried to describe the possible relationship between ET and dental wear patterns in permanent lower first molars (M_1) aiming to observe whether an adaptive response to the environmental and cultural context is detectable. The present work aims to investigate a possible signal of ET adaptive response in M_1 (wear stage 3; Molnar, 1971) belonging to individuals who lived between the Neolithic (early 6th millennium BCE) and the Bronze Age (second half of the 2nd millennium BCE) in Croatia to identify any signal of change in dental tissue proportions based on archaeologically documented shifts in population structure and subsistence strategies. In order to do so, we explored 3D Average Enamel Thickness (AET) of the entire crown and wear pattern distribution among individuals and across chronological groups. We then described a new method called "Enamel Thickness per Masticatory Phases" (ETMP) involving the creation of virtual sections cutting enamel and coronal dentine in three parts based on masticatory phases, and explored the distribution of 3D AET accordingly. Finally, we performed geometric morphometric analysis on dental crown to ascertain possible morphological differences between Neolithic, Eneolithic, and Bronze Age groups. Results show that Bronze Age individuals differ from previous groups due to 1) higher values of ET in both the entire crown and specifically in the buccal area, 2) to an extensive wear pattern localized on the buccal side, and 3) to the distal extension of the hypoconid together with an extended mesio-distal shape of the crown. These patterns may represent an adaptive response of dental tissue to varying functional demands (e.g. archaeologically documented dietary shift). The study of ETMP therefore offers a more nuanced method, in addition to morphology and macrowear analysis, to document biocultural processes of change over time in archaeological populations through dental tissues.

* Corresponding author.
E-mail address: Gregorio.oxilia3@unibo.it (G. Oxilia).

https://doi.org/10.1016/j.jas.2023.105776
Received 27 September 2022; Received in revised form 28 February 2023; Accepted 5 April 2023
Available online 10 April 2023

1. Introduction

Many anthropological studies have examined the functional implications of enamel thickness distribution in the human dental crowns. Although enamel thickness is no longer regarded as a reliable phylogenetic character due to considerable homoplasy (Dumont, 1995; Schwartz, 2000a), taxonomic assessments of the enamel thickness (in a controlled plane of section or using volumetric data) of the earliest putative hominins from eastern Africa (e.g., Kono and Suwa, 2008; Smith et al., 2008; Olejniczak et al., 2008b; Olejniczak et al., 2008c; Suwa et al., 2009) and within the genus *Homo* (e.g., Smith et al., 2012; Molnar et al., 1993; Grine et al., 2004; Bayle et al., 2010; Oxilia et al., 2022; Been et al., 2017; Margherita et al., 2017) continue to be relevant.

Hominins are generally considered a thick-enameled clade compared to the thin-enameled extant African apes. Despite this characterization, enamel thickness variation within the genus *Homo* is broader than commonly stated, with Neanderthals occupying the thinner end of this range (e.g. Fornai et al., 2014; Olejniczak et al., 2008a; Martín-Francés et al., 2020).

Thinner enamel in Neandertals has been used to support inferences about life history and general health (Smith and Zilberman, 1994; Zilberman et al., 1992; Smith and Zilberman, 1994, Ramirez Rozzi, 1996). Moreover, a trend in enamel thickness has been identified for the later undisputed hominins including *H. sapiens*. In particular, the latter seems to be defined by a relatively thick enamel tissue distally from first to third molar (Schwartz 2000a, 2000b; Macho and Berner 1993) and differences in enamel thickness characterizing 'functional' (buccal side thicker) and 'supporting' (lingual side thinner) cusps (Molnar and Gantt 1977; Schwartz 2000a, 2000b; Macho and Berner 1993, 1994). These trends seem to be due to a unique odontogenetic process induced by an extreme dental reduction (Grine et al., 2001; Grine 1991; Spoor et al., 1993) as well as a functional model of masticatory biomechanics (Koolstra et al., 1988; Schwartz 2000a, 2000b; Macho and Berner 1993, 1994) where the posterior molars and functional cusps have been predicted to encounter higher occlusal forces (Sathyanarayana et al., 2012; Sonnesen and Bakke, 2005; Khadijah et al., 2020) producing a response in enamel thickness.

Following early contributions based on the physical sectioning of the tooth (e.g. Grine, 2005, 2002; Martin, 1985), several 2D and mainly 3D digital methods (Smith et al., 2005, 2006; Olejniczak and Grine, 2006; Olejniczak et al., 2008a; Benazzi et al., 2014; Kono et al., 2002; Vazzana et al., 2018) have been developed to provide accurate and more precise quantification of dental enamel thickness, thus representing a consistent analytical method that in addition prevents physical damage of the specimens.

Molars are the main dental class investigated for enamel thickness and mineralized tissue proportion (Grine, 2002, 2005; Kono et al., 2002; Olejniczak et al., 2008a; Fornai et al., 2014; Skinner et al., 2015) because considered a key of occlusion and of significant impact on the future occlusion health (Ebrahimi et la. 2010). Hominin molar enamel thickness is a good marker reflecting selection for functional adaptation against macrowear (Janis and Fortelius, 1988; Shellis, 1998). Indeed, macrowear has been considered as a physiological phenomenon of dental tissue loss linked to dietary habits (El Zaatari et al., 2011; Fiorenza et al., 2018; Fiorenza and Kullmer, 2013; Hinton, 1982; Kaidonis et al., 1993; Molnar, 1971; Oxilia et al., 2021a; Smith, 1984), to predominant occlusal movements performed during masticatory and parafunctional activities (Benazzi et al., 2013a; Kullmer et al., 2009, 2013; Oxilia et al., 2015, 2017, 2018; Traversari et al., 2019), and to biomechanical effects of occlusal loading (Benazzi et al., 2011, 2013b, 2013c, 2015, 2016; Dejak et al., 2003). It has been shown that enamel thickness in molars differs even in modern human populations when considering different time periods (e.g. Le Luyer et al., 2014) and/or tooth type, sex, and population (Smith et al., 2006).

At present, however, the exact relationship between enamel thickness and the distribution of dental wear pattern across different masticatory phases has not yet been thoroughly investigated, and there is no systematic evidence that could directly link enamel thickness distribution with change over time in subsistence and masticatory activities due to wide alterations (masticatory and paramasticatory activities as well as asymmetries) affecting the stability of our masticatory system and, thus, dental tissues. The present work aims to explore significant differences in enamel thickness between different masticatory phases using 3D data on moderately worn permanent lower first molars. At the same time, we aim to recognize potential patterns of variability over time linked to change in diet, subsistence strategy by analysing the distribution of enamel thickness across different masticatory phases and dental crown shape in Neolithic, Eneolithic, and Bronze Age individuals uncovered in present-day Croatia (see *section 2.1*). The absence of differences would suggest that the distribution of enamel thickness is not linked to or affected by either masticatory activities or by the anthropological/socioeconomic changes documented by archaeologists in the analysed chronological contexts (Varalli et al., 2022).

In order to do so, we first used 3D enamel models for each sampled tooth to calculate Average Enamel Thickness (AET) for the entire dental crown and obtained a distribution of AET values for each chronological group. We then proceeded by identifying and quantifying the extension of macrowear per each masticatory phase (Buccal Phase I, Lingual Phase I and Phase II) in each sampled tooth, and developed a new 3D virtual method (Enamel Thickness per Masticatory Phases; hereafter ETMP) involving the creation of virtual sections passing through dentine and enamel tissues useful to obtain enamel volume and Enamel-Dentine Junction surface (used for the computation of the 3D AET) for each masticatory phase.

In order to reduce the possible influence of time and genetic diversity within each sampled group, archaeological contexts of interest were selected based on four criteria: 1) precise chronology and association with diagnostic material culture; 2) sampled individuals had to be uncovered in the same or geographically close sites; 3) the preservation of skeletal/dental remains had to be excellent; and 4) presence and consistency of information on the dietary patterns of each of the analysed populations (through archaeological proxies e.g. carbon and nitrogen stable isotopic analysis). With that in mind, we chose the assemblages from three different time periods from modern-day Croatia: the Neolithic (Jagodnjak/Beli Manastir), the Eneolithic (Potočani) and the Bronze Age (Bezdanjača Cave) (Fig. 1).

2. Material and methods

The sample consists of permanent lower first molars (M1) with similar wear stage (equal to 3 based on Molnar, 1971) of 25 individuals from the four archaeological sites: Jagodnjak (n = 1), Beli Manastir (n = 9), Potočani (n = 9), and Bezdanjača (n = 6) (Table 1) represented by male (n = 11), female (n = 12) and two individuals for which sex was not available (NA). Dental crowns characterized by pathological signs and taphonomic alterations were excluded from current analyses, while individuals with uncertain sex attribution were not selected to test differences between sexes. We selected teeth characterized by Y groove pattern and five cusps respectively to avoid any influence induced by morphological features.

2.1. Archaeological setting

Jagodnjak is a site in eastern Croatia, in Osijek-Baranja County, north of the city of Osijek. Rescue excavations that took place in 2014/2015 at the Krčevine location, revealed archaeological strata from the Neolithic, Bronze Age, Late Iron Age, Roman and Early Medieval periods (Tresić Pavičić, 2015). Among other features, several Early Neolithic Starčevo culture burials have been excavated. Three direct radiocarbon dates put the use of the Starčevo culture burials to the early 6th millennium BCE (PSUAMS 4442: 6895+/25 BP, 5838–5726 cal BCE; PSUAMS 4443: 6925+/25 BP, 5876–5735 cal BCE PSUAMS 4445:

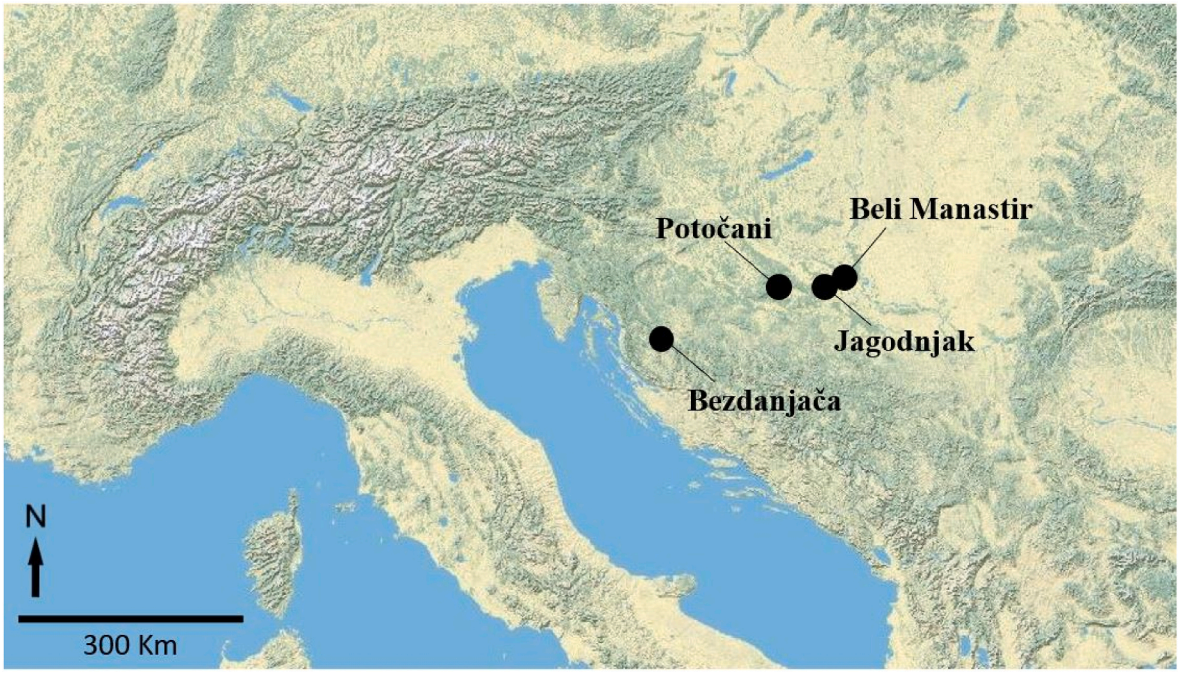

Fig. 1. Map showing the geographic location of the sites analysed in the study (base map credit: USGS National Map Viewer, http://viewer.nationalmap.gov/viewer/).

6965+/25 BP, 5968–5757 cal BCE). Two of the burials can be defined as "mass" burials containing several commingled skeletons with four additional individual inhumations. In each of the four inhumations the individuals were buried in pits within the settlement, lying in a flexed position on their side. The sample used in this analysis comes from burial 79 defined as a "mass grave" as it contained commingled remains of at least four young adult males. Genomic as well as C/N isotopic data suggest this was a homogenous community with the diet mostly based on C3 resources with a low intake of animal protein (Novak, unpublished data).

The site of Beli Manastir – Popova zemlja is located in eastern Croatia, in Osijek-Baranja County, between Drava and Danube rivers. Rescue excavations due to the construction of a motorway, conducted in 2014 and 2015, revealed a multi-stratigraphic site with the archaeological sequence starting with the Neolithic Starčevo, Sopot and Lengyel cultures, continuing with Eneolithic Baden and Vučedol cultures and ending with the Roman period (Los, 2020). In addition to the various phases of the prehistoric settlement and cemetery as well as two Roman period brick kilns nearly 47,000 pottery fragments, bone objects, stone tools and animal bones were recorded and excavated (Los, 2020). Some burials were discovered at the top of the structure fills, which means that spaces inside the structures were used for burials after losing their original function. However, most burials were found at the very bottom of the structures (i.e. pit houses), along their edges. Nevertheless, some inhumations were recovered from the bottom of the pits and at the bottom of the channel running along the eastern edge of the site. Most of the recovered burials were in a contracted position on their left or right sides in various orientations (mostly SW-NE), and some had ceramic vessels placed by their head. The skeletons in the channel were found in an unarranged extended supine or prone position with no addition of grave goods except for some animal bones (Los, 2020). A series of direct radiocarbon dates place the analysed burials to the Neolithic period, e.g. to the 6th and the first half of the 5th millennium BCE (for more details see Freilich et al., 2021; Jovanović et al., 2021a; Los, 2020). Most of the skeletons were complete, and only a few were missing some osteological elements due to recent human activity such as ploughing. In total, 39 individuals were available for the analysis: 17 subadults, 11 females and 11 males. The bioarchaeological analysis of this skeletal assemblage indicates that: (i) this was a typical Neolithic population heavily dependent on agriculture, (ii) its members suffered from poor subadult health, (iii) it was a community that experienced a low level of interpersonal violence (Novak, 2017). Carbon and nitrogen stable isotopes analysis conducted on several individuals showed that "their diet was consistent with typical Early and Late Neolithic dietary patterns in the region, showing that they consumed terrestrial resources (C3 plants, domesticates and wild game) with no isotopic evidence for the use of aquatic food" (Jovanović et al., 2021a). And finally, ancient DNA analysis was performed on the remains of 19 Neolithic individuals from the site showing strong genetic continuity from the Early Neolithic and the evidence of first cousin mating practices (Freilich et al., 2021).

The sample from Potočani was discovered in 2007 during a field survey near the town of Požega in continental Croatia as the erosion caused by heavy rain uncovered a part of the circular pit (approximately 2 m in diameter and about 1 m in depth) containing commingled, in certain cases still articulated, remains of a large number of people (Potrebica and Balen, 2008). The position of the articulated remains indicates that the bodies were thrown into the pit randomly, without any care. Radiocarbon dates from three human bones, taken at various levels in the pit, gave results of around 4200 years cal BCE (Beta 233122: 5240+/40 BP; Beta 233123: 5310+/40 BP; UCIAMS 140250: 5325+/20 BP (Jovanović et al., 2021; McClure et al., 2020). Although only few diagnostic pottery fragments were found in the pit, the timeframe fits within the Lasinja culture of the Middle Copper Age (Balen, 2008). Bioarchaeological analyses of the sample suggest a minimum of 41 people of both sexes and age range between approximately two and 50 years of age at death are present (about half of the individuals are subadults below 18 years of age). Interestingly, thirteen crania display perimortem injuries (with a total of 28 injuries), ranging from blunt force trauma, cuts, and piercing injuries (Jovanović et al., 2021). The indiscriminant pattern of injuries does not follow a specific pattern of age and sex, as the injuries were observed in one boy 2–5 years old, one girl 6–10 years old, three boys and one girl 11–17 years old, five younger adults (18–35 years; one male and four females), and two middle-aged males (36–50 years) (Jovanović et al., 2021). In addition, most of the injuries are located on the lateral, posterior, or superior parts of the crania and no so-called defensive wounds have been observed on

Table 1
Sample composition.

Time period	Sample	Site	Sex[a]/age	$\delta^{13}C/\delta^{15}N$ (in ‰)	MicroCT scan
Neolithic	G79	Jagodnjak Krčevine	Male, 20–35 years	−20.6/10.6	DPES (Ferrara, Italy)
Neolithic	G9	Beli Manastir Popova zemlja	Female[a], 13–15 years	NA	DPES (Ferrara, Italy)
Neolithic	G27	Beli Manastir Popova zemlja	Female[a], 30–38 years	NA	DPES (Ferrara, Italy)
Neolithic	G2	Beli Manastir Popova zemlja	Female[a], 12–14 years	−19.2/9.5	ICTP (Trieste, Italy)
Neolithic	G7	Beli Manastir Popova zemlja	Male[a], 18–26 years	NA	ICTP (Trieste, Italy)
Neolithic	G16	Beli Manastir Popova zemlja	Female[a], 9–11 years	NA	ICTP (Trieste, Italy)
Neolithic	G30	Beli Manastir Popova zemlja	Male[a], 20–26 years	NA	ICTP (Trieste, Italy)
Neolithic	G36	Beli Manastir Popova zemlja	Male[a], 12–13 years	NA	ICTP (Trieste, Italy)
Neolithic	G1	Beli Manastir Popova zemlja	NA, 7–9 years	−19.6/9.4	ICTP (Trieste, Italy)
Neolithic	G4	Beli Manastir Popova zemlja	Male[a], 12–14 years	−19.4/9.1	ICTP (Trieste, Italy)
Eneolithic	P8L12	Potočani	Male[a], 10–15 years	−19.8/10.2	DPES (Ferrara, Italy)
Eneolithic	P8L8-3	Potočani	Male[a], 10–15 years	−20.0/11.9	DPES (Ferrara, Italy)
Eneolithic	P8L3-3	Potočani	Male[a], 10–15 years	NA	DPES (Ferrara, Italy)
Eneolithic	P42	Potočani	Female[a], 20–35 years	−19.9/10.3	ICTP (Trieste, Italy)
Eneolithic	P1	Potočani	Female[a], 10–15 years	−20.0/10.7	ICTP (Trieste, Italy)
Eneolithic	P10	Potočani	Female[a], 20–35 years	−19.9/11.2	ICTP (Trieste, Italy)
Eneolithic	P41	Potočani	Male[a], 10–15 years	−19.4/10.4	ICTP (Trieste, Italy)
Eneolithic	P46	Potočani	Female[a], 10–15 years	−20.2/10.8	ICTP (Trieste, Italy)
Eneolithic	P47	Potočani	Male[a], 10–15 years	−20.0/9.9	ICTP (Trieste, Italy)
BronzeAge	BZV_5	Bezdanjača Cave	Female[a], 25–35 years	−17.1/8.8	ICTP (Trieste, Italy)
BronzeAge	BZV_21 E	Bezdanjača Cave	NA, 12–18 years	NA	ICTP (Trieste, Italy)
BronzeAge	BZV_33C	Bezdanjača Cave	Female[a], 20-35	NA	ICTP (Trieste, Italy)
BronzeAge	BZV_33 P	Bezdanjača Cave	Female[a], 12–18 years	NA	ICTP (Trieste, Italy)
BronzeAge	BZV-33 L	Bezdanjača Cave	Female[a], 12–18 years	NA	ICTP (Trieste, Italy)
BronzeAge	BZV-33 R	Bezdanjača Cave	Male[a], 15–20 years	NA	ICTP (Trieste, Italy)

DPES = Department of Physics and Earth Sciences; ICTP = Abdus Salam International Centre of Theoretical Physics.
[a] Molecular sex established by means of ancient DNA.

postcranial remains. All this combined strongly suggests a single episode of violent encounter and execution of a small community during the Middle Copper Age (Janković et al., 2021; McClure et al., 2020; Novak et al., 2021). N/C stable isotopes analysis of this catastrophic assemblage indicate higher than expected nitrogen values in comparison with other regional populations and significant differences between children, juveniles, and adults from the site (McClure et al., 2020). On the other hand, aDNA study indicates that: "(i) the majority of individuals were unrelated and instead were a sample of what was clearly a large farming population, (ii) the ancestry of the individuals was homogenous which makes it unlikely that the massacre was linked to the arrival of new genetic ancestry, and (iii) there were approximately equal numbers of males and females" (Novak et al., 2021).

The cave of Bezdanjaca is located on the north-eastern side of the Vatinovac Hill near Vrhovine in Lika region of Croatia. The entrance is funnel-shaped, 30 × 12 m wide, with a 31-m vertical drop. It was first discovered by speleologists in 1960 and subsequent archaeological work in the cave in 1965 resulted in numerous archaeological remains (pottery, metal items and other finds) that cluster into two distinct periods of the Bronze Age (Malez, 1967, 1979; Malinar, 1976). According to (Drechsler-Bižić, 1979), the site was used during the Middle Bronze Age (Horizon I, Br C/D), and Late Bronze Age (Horizon II, Br D/Ha A) (Drechsler-Bižić, 1979). Recently, this was confirmed by a series of direct radiocarbon dates placing the use of this necropolis to the second half of the 2nd millennium BCE (for more details see Lazaridis et al., 2022; Zavodny et al., 2017. A total of 57 separate grave units were discovered, with the remains of about two hundred people (Drechsler-Bižić, 1979). Ten graves contained more than one deceased (five to 20 individuals). The significance of the human skeletal remains was evident immediately after discovery, but only preliminary analyses or analyses of a limited scope of human skeletal material have been carried out so far (Boljunčić, 1991, 1997; Janković and Novak, 2021; Malez, 1973; Malez and Nikolić, 1975; Percač, 1992; Šlaus, 2002). Bioarchaeological analysis of the preserved remains showed equal representation of both sexes (ten skulls belong to female and ten to male individuals; four less preserved crania probably also belong to males and another skull to a female individual; it was not possible to establish the sex for one skull). In addition to adults, seven older children and two adolescents are also present in the sample. Several adult crania show evidence of perimortem injuries while one cranium exhibits traces of a neurosurgical intervention–trephination–that the individual survived and recovered from (Carić et al., 2020). Results of the stable isotope analysis reveal that the individuals from Bezdanjaca consumed notable quantities of C4 plants during their childhood (most likely millet) (Martinoia et al., 2021). Genomic analysis on 35 individuals showed interesting results, as ten of the individuals clustered in four families (Lazaridis et al., 2022).

2.2. Micro-CT scan and digital reconstruction

High-resolution micro-CT based digital volumes were measured by microfocus X-ray computed tomography (μCT) at the Multidisciplinary Laboratory of the Abdus Salam International Centre of Theoretical Physics – ICTP (Trieste, Italy) (N = 19, see Table 1) using a system specifically designed for the study of paleontological and archaeological materials (Tuniz et al., 2013) and at the Department of Physics and Earth Sciences, University of Ferrara, Ferrara, Italy (N = 6) using a dedicated μCT system for the acquisition of small samples.

The μCT acquisitions performed at the ICTP of the specimens were carried out by using a sealed X-ray source (Hamamatsu L8121-03) at a voltage of 110 kV, a current of 90 μA and with a focal spot size of 5 μm. The X-ray beam was filtered by a 0.1 or 0.05 mm-thick copper absorber. A set of 1440 projections of the samples were recorded over a total scan angle of 360° by a flat panel detector (Hamamatsu C7942SK-25) with an exposure time/projection of 1–2 s.

The resulting μCT slices were reconstructed using the commercial software DigiXCT (DIGISENS SAS) in 32-bit format and obtaining an isotropic voxel size of 20–30 μm.

The micro-CT images performed at the University of Ferrara were carried out by using a microfocus X-ray tube (Hamamatsu L9421-02), a rotation stage and a flat panel detector (Hamamatsu C14400DK-51). All the data acquisitions have been performed at a voltage of 80 kVp, 100 μA and a focal spot size of nearly 5 μm. The X-ray beam has been filtered by 150 μm copper. A set of 360 images over an angular scan of 360° have been acquired of each sample with an integration time of 100ms. The planar images have been dark and flat corrected and reconstructed using a home-made software in a 3D volume with an isotropic voxel of 30 μm.

The micro-CT images of the original samples were virtually segmented using Avizo 2021.2 software (Thermo Fisher Scientific, Waltham, Massachusetts, US). The segmented enamel caps and virtually filled dentins were converted to meshes using Geomagic Design X (3D Systems Software, Rock Hill, South Carolina, US).

2.3. 3D Enamel thickness

To calculate the 3D enamel thickness, we followed the guidelines provided by Benazzi et al. (2014) for molars. The crown was separated by the root using the interpolated surface of the cervical line (Benazzi et al., 2014). We measured: the enamel volume (mm^3) and the enamel-dentine junction (EDJ) surface (mm^2). These measurements were used for the computation of the 3D average enamel thickness index (3D AET = volume of enamel divided by the EDJ surface; index in millimeters) (e.g. Benazzi et al., 2014).

2.4. Dental macrowear analysis

Dental macrowear refers to general dental tissue loss resulting in the alteration of the macroscopic morphology of the occlusal relieves of the crown that, within stage 3 worn teeth, it is still possible to recognize and quantified the greatest distribution of wear pattern. Occlusal wear facet areas of M_1s were identified and analysed using the occlusal fingerprint analysis (OFA) method. The facets were manually mapped on each digital surface model and labelled according to the numbering system created by Maier and Schneck (1981) and later modified by Kullmer et al. (2009).

In hominins, during mastication, the power stroke is divided into two phases (Hiemae and Kay, 1972; Kay and Hiiemae, 1974): the first (Phase I, divided in Lingual and Buccal) happens when opposite molar cusps tend to slide past each other moving to centric occlusion (maximum intercuspation). The second phase (Phase II) is an anterior-medial movement, where the lower molars move out of occlusion. The chewing cycle terminates with the opening of the jaw. The relative surface area of the wear facets attributed to Buccal Phase I (BPI), Lingual Phase I (LPI), and Phase II (PII) of the occlusal power stroke was computed by summing the absolute areas (in mm^2) belonging to the same phase and dividing this sum by the total occlusal wear area (BPI, LPI, PII, respectively).

2.5. Enamel thickness per masticatory phases (ETMP)

In this contribution we propose a new method to compute and analyse enamel thickness distribution for each masticatory phase. In detail, each tooth was oriented in Geomagic Design X 3D software by placing the best-fit plane computed at the cervical line (i.e., the cervical plane that best fits a spline curve digitized at the cervical line) parallel to the xy-plane of the Cartesian coordinate system (e.g., Benazzi et al., 2012). The 3D digital crown models were then rotated around the z-axis in order to have the mesiodistal fissure parallel to the x-axis.

Once wear patterns for the different masticatory phases (Buccal Phase I, Lingual Phase I and Phase II) were identified, the separation margins of each masticatory phase were obtained by using virtual spline both on the enamel, following the wear pattern (Fig. 2A), and on the dentine (Fig. 2B), following anatomical morphology of dentine horns (buccal area) and lingual grooves (lingual area). The splines (Fig. 2C) were projected on virtual planes created parallel (Occlusal offsets, Fig. 2C; and Periapical Offset, Fig. 2D) to the cervical plane, in order to obtain two virtual sections (Buccal and Lingual) passing through dentine and enamel tissues. Finally, the three different parts of the crown (Fig. 2E) were used to measure the enamel volume and EDJ surface. These measurements were used for the computation of the 3D AET for each masticatory phase (i.e., B_AET, PII_AET, and L_AET, respectively).

2.6. Geometric morphometric (GM) analysis

A 3D template of 59 (semi)landmarks (9 anatomical landmarks, 20 curve semilandmarks and 30 surface semilandmarks) was created in Viewbox 4 (dHAL software) (Fig. 3) and subsequently applied to the targets. The semilandmarks were allowed to slide on the curves (curves semilandmarks) and on the surface (surface semilandmarks) to minimize the thin-plate spline (TPS) bending energy between the target and the template (Gunz and Mitteroecker, 2013; Slice, 2006).

The (semi)landmark coordinates were allowed to slide against recursive updates of the Procrustes consensus (Gunz et al., 2005; Mitteroecker and Gunz, 2009; Slice, 2006) and converted into shape coordinates, with scale, position and orientation standardized via Generalized Procrustes Analysis (GPA) (Rohlf and Slice, 1990; Slice, 2006) using the R package "geomorph" (Adams and Otárola-Castillo, 2013) in R version 4.1.0 (R Core Team, 2021). A shape-space Principal Component Analysis (PCA) was performed on the Procrustes coordinates to explore the pattern of morphological variation across the sample. Visualization of shape changes along the principal axes was obtained by TPS deformation of the Procrustes grand mean shape surface in Avizo 2021.2.

2.7. Univariate and multivariate statistical analysis

Because of small sample size, which makes it difficult to test for violation of parametric assumptions, we used non-parametric and permutational tests to ascertain the presence of potential differences between sexes within groups, and among chronological groups (i.e. Neolithic, Eneolithic, and Bronze Age). Sex was considered as a potential driver of enamel thickness variability as proposed by Hlusko et al. (2004) and Macho and Berner (1993). Differences were ascertained in the pooled sample (without considering chronology) using two-tailed Kruskall-Wallis test and Dunn test to measure differences between males and females in 3D AET for the entire crown as well as for each masticatory phase (Buccal Phase I, Lingual Phase I, and Phase II). The impact of sex on the distribution of crown shape in the same pooled sample was instead investigated using Permutational Multivariate Analysis of Variance (PERMANOVA) through the function adonis in the

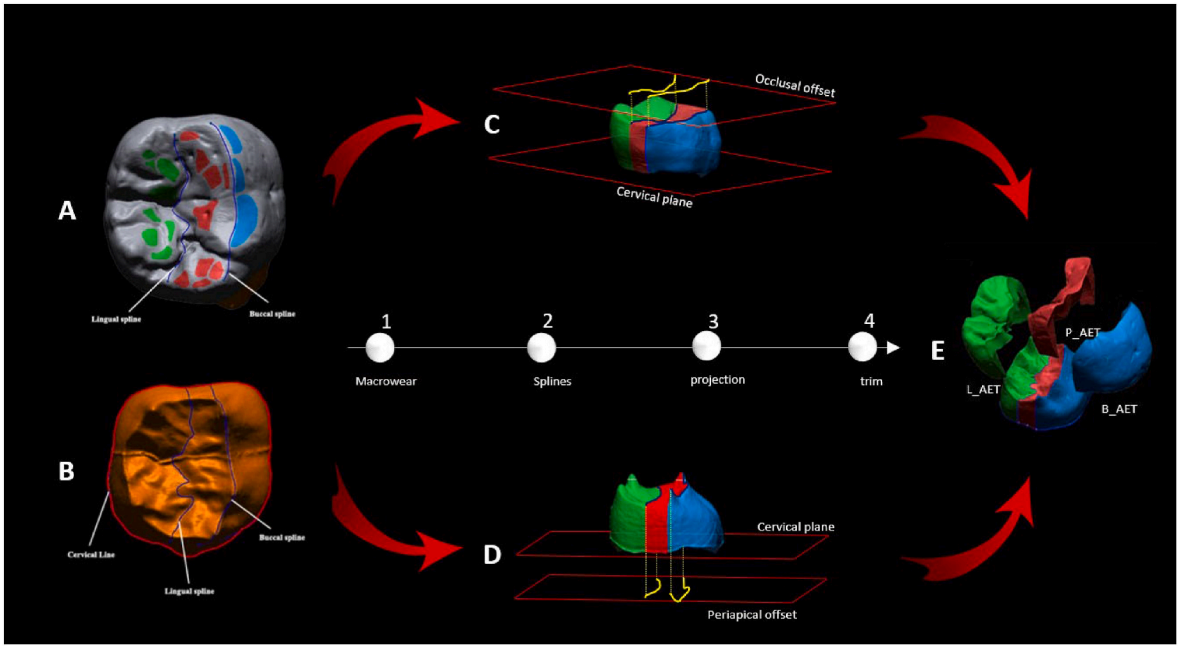

Fig. 2. ETMP method. A) Identification of virtual spline both on the enamel, following the wear pattern (A), and on the dentine (B), following anatomical morphology of cusp and lingual grooves. Splines were then projected on two planes (occlusal C, and periapical D) parallel to the cervical plane. Enamel and coronal dentine volumes were virtually separated (E) according to masticatory phases (blue = Buccal Phase I; green = Lingual Phase I; red = Phase II). (For interpretation of the references to colour in this figure legend, the reader is referred to the Web version of this article.)

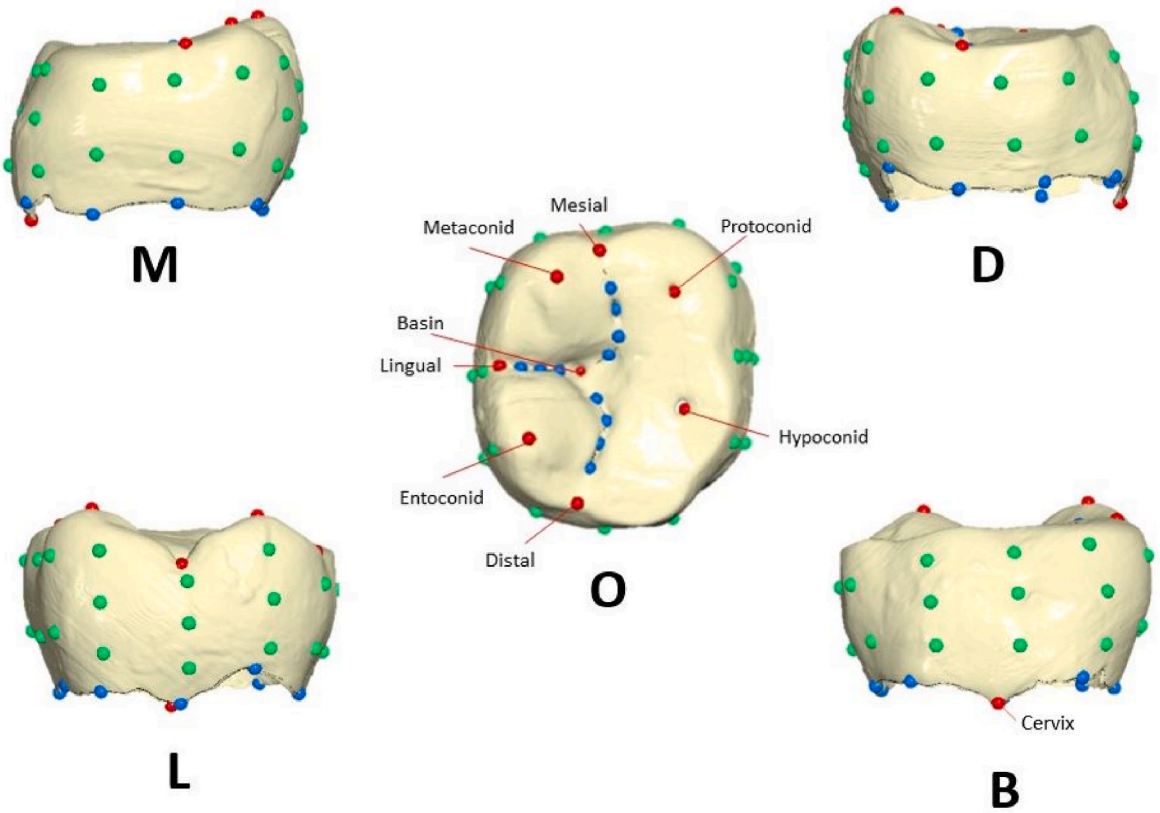

Fig. 3. Template with landmarks (red), curve and surface semilandmarks (blue and green, respectively) digitized on a dental crown. (For interpretation of the references to colour in this figure legend, the reader is referred to the Web version of this article.)

package vegan in R.

We then focused on variability in 3D AET within each chronological group and between pairs of chronological groups. We used the same univariate methods (two-tailed Kruskal-Wallis and Dunn test) to identify potential in-group differences between Buccal Phase I, Lingual Phase I, and Phase II. At the same time, we investigated between-group differences in the distribution of 3D AET both at crown scale and at a masticatory phase scale. Bonferroni correction was used to mitigate the effects of multiple testing. To support and better interpret the obtained results, we explored the distribution of dental macrowear across Buccal Phase I, Lingual Phase I, and Phase II of each chronological group through a ternary diagram, in order to connect potential differences in 3D enamel thickness to the potential effect of e.g. dietary habits and crown morphology. To further investigate the latter, we used an approach based on Geometric Morphometrics. We first computed a Procrustes distance matrix (Dryden et al., 1998; Rohlf and Slice, 1990) between all the configurations obtained as per the procedure described in the Geometric Morphometric section. We then calculated the multivariate dispersion of each group and tested if group variances were homogeneous using the function betadisper in the vegan package in R (Anderson, 2001). We finally used PERMANOVA to assess whether the distribution of Procrustes distances – and therefore of different morphologies – was significantly different among the three chronological groups.

3. Results

Even though the entire crown of females shows higher values of AET (Fig. S1), no significant differences were found either for the global value (Fig. S1a) (chi-squared = 2.3674, df = 1, p-value = 0.1239) or per masticatory phases (Fig. S1b). Moreover, the influence of sexual dimorphism on distribution of the wear pattern (Fig. S2) was excluded for both Buccal Phase I (chi-squared = 0.9697, df = 1, p-value = 0.3248) and Lingual Phase I (chi-squared = 0.37879, df = 1, p-value = 0.5383) as well as Phase II (chi-squared = 0.64015, df = 1, p-value = 0.4237). Finally, the shape-space PCA plot of the pooled sample shows a considerable degree of overlap between males and females (Fig. S3; Table S1 and Table S2). For the reason described above, the entire sample was considered as a unique group and explore variability only across chronological groups.

Values of 3D AET both for the entire crown and per masticatory phases of each individual for all time periods are reported in Table 2 and Fig. 4. Enamel thickness belonging to the Neolithic individuals are significantly lower than those obtained for Bronze Age (chi-squared = 6.9298, df = 2, p-value = 0.03128) (Fig. 4A), which also shows the highest values of Buccal AET significantly different than the other masticatory phases (chi-squared = 9.0122, df = 2, p-value = 0.01104; Fig. 4B).

Abbreviation: AET = Average Enamel Thickness; BPI= Buccal Phase I wear; PII= Phase II wear; LPI = Lingual Phase I wear; B_AET = Buccal Average Enamel Thickness; PII_AET = Phase II Average Enamel Thickness; L_AET = Lingual Average Enamel Thickness. See Table S3 for raw data used to determine 3D AET, BAET, LAET, PIIAET indexes.

The distribution of wear patterns is characterized by high values of Lingual Phase I facets (Table 2). Neolithic (BPI average: 0.17) exhibits the lowest value of Buccal Phase I wear when compared to Eneolithic (BPI average: 0.18) and Bronze Age (BPI average: 0.29) (Fig. 5). Buccal Phase I is the only masticatory phase that, even after Bonferroni correction, exhibits significant differences between the Bronze Age and other groups (chi-squared = 7.1268, df = 2, p-value = 0.02834).

The first two PCs account for 41% of the total variance and contribute to separating groups belonging to different time periods. Betadisper shows homogeneity of group variances (Table 3), and PERMANOVA results show significant differences between Bronze Age individuals and the other examined groups (Table 4). Morphological differences are observed in the extreme shape of the PC1 and PC2 axes, in particular the protoconid cusp is more expanded on positive PC1 and reduced on negative PC1.

Differently was observed for hypoconid and hypoconulid that appear distally extended on positive PC1 and reduced on negative PC1. Concerning positive PC2, it accounts for the relative mesio-distal expansion of the crown, while negative PC2 is related to a more rounded crown (Fig. 6). Overall, results in the shape space PCA suggest that there are differences driven by crown morphology of the populations considered in this study where Bronze Age individuals appear more separated than the other groups (Neolithic and Eneolthic individuals), which instead are overlapped.

Table 2
3D values of enamel thickness, wear pattern, enamel and dentine volume for each individual.

Sample	Time_period	Sex	AET	BPI	PII	LPI	B_AET	PII_AET	L_AET
G79	Neolithic	Male	0.83	0.21	0.31	0.49	0.87	1	1.13
G9	Neolithic	Female	1.17	0.23	0.48	0.28	1.23	0.73	0.75
G27	Neolithic	Female	0.92	0.12	0.26	0.62	0.36	1.12	0.87
G2	Neolithic	Female	0.91	0.25	0.21	0.54	0.87	1.81	0.96
G7	Neolithic	Male	1.07	0.08	0.56	0.36	1025	0.89	0.83
G16	Neolithic	Female	0.91	0.1	0.53	0.37	1	1.03	1.01
G30	Neolithic	Male	0.77	0.07	0.43	0.5	0.71	1.51	1.09
G36	Neolithic	Male	0.81	0.11	0.4	0.49	0.81	1.32	1.14
G1	Neolithic	NA	0.87	0.32	0.25	0.43	0.83	0.73	1.05
G4	Neolithic	Male	0.96	0.17	0.5	0.33	0.93	1.17	0.84
P8L12	Eneolithic	Male	1.65	0.24	0.44	0.32	1.55	0.53	0.62
P8L8-3	Eneolithic	Male	1.03	0.19	0.38	0.43	1.78	0.84	0.97
P8L3-3	Eneolithic	Male	0.84	0.23	0.41	0.37	0.69	0.83	1.15
P42	Eneolithic	Female	0.91	0.05	0.67	0.27	0.91	1.27	1.04
P1	Eneolithic	Female	0.88	0.2	0.15	0.65	0.77	1.05	1.06
P10	Eneolithic	Female	1.06	0.18	0.38	0.44	1.02	1.04	0.88
P41	Eneolithic	Male	0.92	0.19	0.45	0.36	0.84	1.11	1.01
P46	Eneolithic	Female	1.09	0.11	0.61	0.27	1.05	0.91	0.88
P47	Eneolithic	Male	0.88	0.15	0.36	0.49	0.8	1.21	1.04
BZV_5	Bronze Age	Female	1.04	0.35	0.34	0.31	0.92	0.9	0.89
BZV_21 E	Bronze Age	NA	1.22	0.09	0.48	0.43	1.1	0.82	0.75
BZV_33C	Bronze Age	Female	1.28	0.35	0.27	0.37	1.25	0.79	0.76
BZV_33 P	Bronze Age	Female	1.25	0.33	0.33	0.34	1.19	0.77	0.77
BZV-33 L	Bronze Age	Female	1.03	0.32	0.45	0.23	1.05	0.97	0.97
BZV-33 R	Bronze Age	Male	0.99	0.32	0.4	0.28	0.98	1.01	0.96

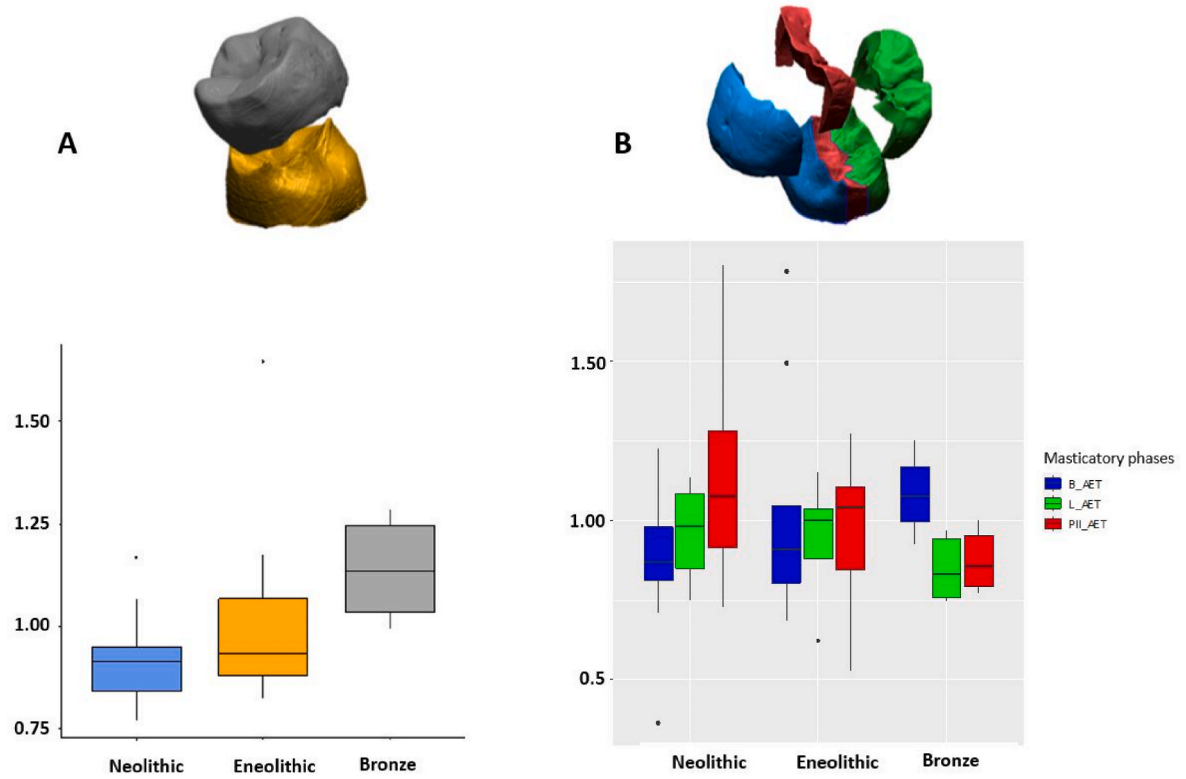

Fig. 4. 3D average enamel thickness (3D AET, mm) box plots (standard deviation interquartile method) for lower first molar at wear stages 3 for chronological and sex variables of entire dental crown (A) and per masticatory phases (B). B_AET = Buccal Average Enamel Thickness; L_AET = Lingual Average Enamel Thickness; PII_AET = Phase II Average Enamel Thickness.

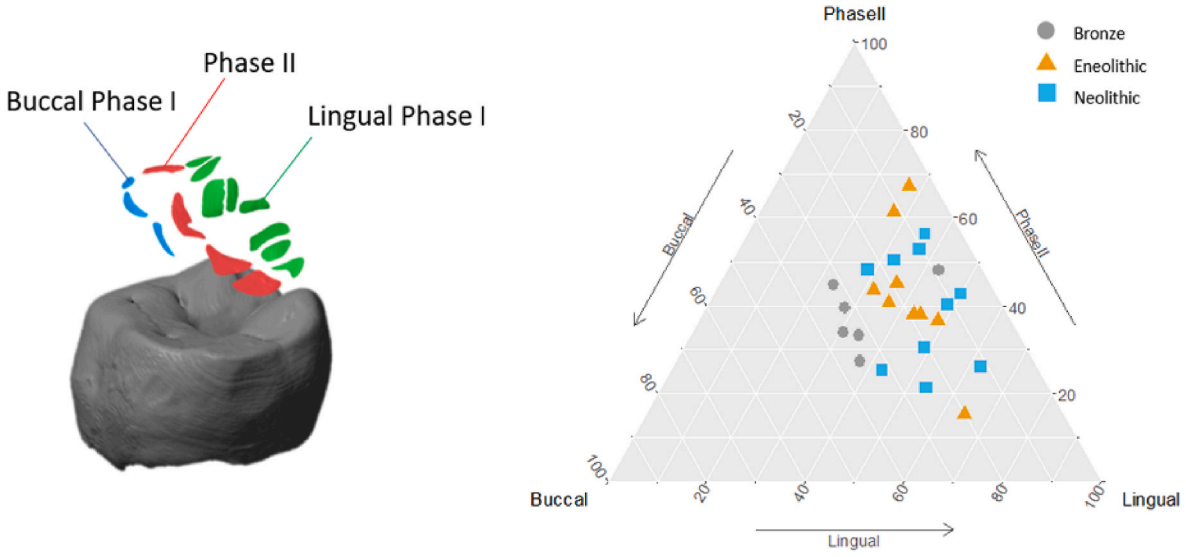

Fig. 5. Ternary diagrams showing the proportions (in %) of relative wear surface of Buccal Phase I areas, Lingual Phase I areas, and Phase II areas (Kay and Hiiemae, 1974), which are positioned in an equilateral triangle. Each base of the triangle represents a ratio of 0% while the vertices correspond to a percentage of 100%. Our chronological groups were identified in the ternary plots as blue (Neolithic), orange (Eneolithic) and grey (Bronze Age) points. (For interpretation of the references to colour in this figure legend, the reader is referred to the Web version of this article.)

Table 3
Permutation-based test of multivariate homogeneity of group dispersions.

	Df	SumOfSqs	MeanSqs	F	N.Perm	Pr (>F)
Groups	2	0.000855	0.000428	0.7586	999	0.486
Residuals	22	0.012401	0.000564			

4. Discussion

Human dental remains are often retrieved as isolated elements in both paleoanthropological and archaeological contexts, and consequently they have been the focus of several scientific contributions for taxonomical identification, dietary and cultural habits as well as biological profile (Margherita et al., 2017; Oxilia et al., 2018, 2022;

Table 4
Results of one-way permutational multivariate analysis of variance (PERMANOVA).

	Df	SumOfSqs	MeanSqs	F.Model	R2	Pr (>F)
Groups	2	0.019577	0.0097883	1.9369	0.14972	0.012 *
Residuals	22	0.111176	0.0050535		0.85028	
Total	24	0.130753			1.00000	

Romandini et al., 2020). Indeed, it is broadly accepted that the enamel thickness and occlusal wear patterns are good indicators for shifting dietary patterns given their presumed functional, phylogenetic, and taxonomic significance (Bortolini et al., 2021; Kay, 1975; Kono, 2004; Lucas et al., 2014; Margherita et al., 2016; Martin, 1985; Molnar, 1971; Molnar and Gantt, 1977; Olejniczak et al., 2008a; Oxilia et al., 2018, 2021b, 2021a; Romandini et al., 2020; Schwartz, 2000a).

In this study, we analysed samples representing four archaeological populations from sites of Jagodnjak (n = 1), Beli Manastir (n = 9), Potočani (n = 9), and Bezdanjača (n = 6), dating to Neolithic, Eneolithic, and Bronze Age, respectively (Table 1) indicative of the heart of ancient migration routes through Europe issuing from the same geographical location (Croatia). These sites were suitable for answering our research question due to the fact that they were excavated by using modern excavation techniques and have a comprehensive and precise archaeological context and chronology with a series of direct radiocarbon dates, the preservation of skeletal/dental remains is excellent, the population homogeneity for each of the studied assemblages is verified by ancient DNA analysis. And finally, recent C/N isotopic studies provided ample information on everyday diet and subsistence strategies of these individuals.

We followed a four-step approach, i.e., 1) we explored 3D AET of the entire crown and then 2) wear pattern distribution to assess any discriminatory distribution among individuals; 3) we describe a new method called Enamel Thickness per Masticatory Phases (ETMP) involving the creation of virtual sections which cut the enamel and coronal dentine in three parts according to each masticatory phase (Buccal Phase I, Lingual Phase I and Phase II) used to explore the distribution of enamel thickness (3D AET); 4) we then performed geometric morphometrics analysis on dental crown to investigate the role of shape in determining morphological differences based on chronology. We found that, in the present sample, 3D AET of the entire crown does not differ significantly among sexes, although female individuals exhibit generally higher values than males. As far as diachronic change is concerned, we found differences in AET values between Bronze Age individuals and the other groups, specifically driven by higher values observed for Buccal phase I. It is interesting to note that Bronze Age samples also differ from the others when looking at crown shape. While the latter has been widely used to estimate relationships of biological affinity and kinship among and within populations (Carter et al., 2014; Irish et al., 2014; Paul and Stojanowski, 2015; Sorrentino et al., 2018; Bayle et al., 2010; Fornai et al., 2014; Le Luyer et al., 2014; Mahoney, 2010; Martin, 1985; Molnar and Gantt, 1977; Schwartz, 2000a; Skinner et al., 2015; Smith et al., 2005; Zanolli, 2015), there is at present no archaeological evidence in Bronze Age contexts of Croatia that suggests a process of population replacement or admixture leading to such a

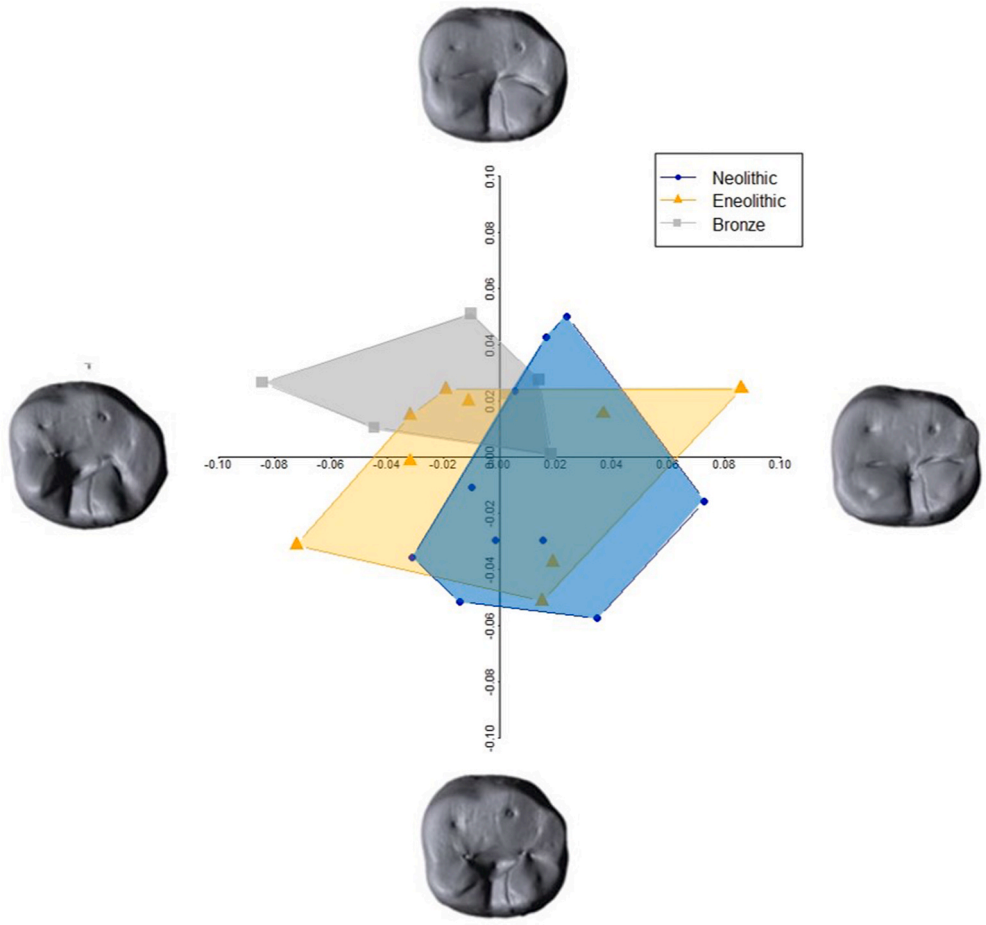

Fig. 6. Shape space PCA plot of the pooled sample and shape warps along axes. Neolithic individuals are in red, Eneolithic individuals in blue and Bronze Age individuals in green. The deformed mean dental crown in the four directions of the PCs are drawn at the extremity of each axis. (For interpretation of the references to colour in this figure legend, the reader is referred to the Web version of this article.)

difference in enamel thickness and dental morphology (Vandkilde et al., 2015; Freilich et al., 2021; Novak et al., 2021) The pattern we document may be therefore interpreted as a result of mechanism that is a functional adaptation induced by shift in nutrition and subsistence.

Several scholars have investigated differences in enamel thickness of molars at a populational level (e.g. Martin, 1985; Macho and Berner, 1993; Schwartz, 2000a, b; Smith et al., 2009b; but see Grine, 2002, 2005; Smith et al., 2006) showing how dietary aspects and masticatory biomechanical constraints may have generated morphological reduction (Hlusko et al., 2004; Horvath et al., 2014; Le Luyer et al., 2014; Pampush et al., 2013; Oxilia et al., 2018) in the outer (enamel) and inner (enamel dentine junction; EDJ) tissue (Skinner, 2008).

Many aspects of diet and behavior can be gleaned from enamel loss. In particular, molar macrowear accumulates during the lifespan of an individual and thus reflects alterations induced by diet, environmental conditions, food-fracture properties, food processing techniques, and cultural habits over long periods (Fiorenza et al., 2018). As documented by Fiorenza et al. (2011), an extended Buccal Phase I may reveal individuals consuming large amounts of tough, fibrous and flat food (also defined as meat-eater human groups), while large Lingual Phase I may characterize individuals who relied on mixed food resources, including a large percentage of hard, abrasive foodstuffs including roots, gums and other plant materials.

Overall, isotopic profiles of the present sample (Novak, 2017; McClure et al., 2020; Jovanović et al., 2021) do not mirror patterns of dental macrowear. In detail, Neolithic sites (Jagodnjak and Beli Manastir) present with the contribution of C3 plant resources with a low intake of animal protein (Novak, unpublished data), as opposed to the Eneolithic site (Potočani), in which higher values of nitrogen were identified (McClure et al., 2020). Bronze Age individuals from Bezdanjaca consumed instead conspicuous quantities of C4 plants (most likely millet, Martinoia et al., 2021; Carić, 2023).

Dental macrowear supports a possible reliance on relatively abrasive plant foods during the Neolithic period, as documented by higher values of macrowear in Lingual Phase I (Fiorenza, 2015; Lucas et al., 2014), while later groups show values of Buccal Phase I macrowear increasing over time, with the highest values recorded during the Bronze Age.

This trend does not seem to be related to either an increased intake of animal protein (unsupported by isotopic values) or to a dietary shift based on an increased reliance on millet (Kirleis et al., 2022; Hasseldine et al., 2017; Janis and Fortelius, 1988; Pechenkina et al., 2002) which during these periods seems to be systematic in Europe and, more particularly, along Atlantic coast (González-Rabanal et al., 2022). However, there is no evidence in the anthropological field (in favor or against) of a specific wear pattern generated by millet consumption, although the highly abrasive effect of ground millet seeds mixed with water on the occlusal dental surface (Saadi et al., 2023) induces a loss of vertical crown dimension and a decrease in masticatory function (Stober et al., 2006). For these reasons, we do not exclude millet consumption as a possible variable of alteration and it is possible that a functional interpretation might be useful to better explain the emerging macrowear and enamel thickness patterns we obtained.

As mentioned above, the high values of enamel thickness we identified in our sample could be supported by functional interpretation of the cusp's role during chewing (a consequence of masticatory stress), which is highest during M1 biting (Mansour and Reynick, 1975; Pruim et al., 1980; Spencer, 1995, 1998) as documented by a number of scholars (e.g., Shillingburg and Grace, 1973; Molnar and Gantt, 1977; Macho and Spears, 1999; Schwartz, 2000a, b; Gantt et al., 2001). Indeed, the "functional/supporting" buccal cusps (protoconid, hypoconid; Schwartz, 2000a; Macho and Spears, 1999) of mandibular molars are mainly involved in crushing and grinding food during chewing, whereas the "non-functional/guiding" lingual cusps (metaconid, entoconid; Spears and Macho, 1995; Macho and Spears, 1999) largely shear food (Kay, 1975; Kay and Hiiemae, 1974). According to Kono et al. (2002), this masticatory dynamic generates a distribution of occlusal enamel which tends to be relatively thicker over the distal lateral side of the buccal area than at its tip or over its occlusal aspect. During maximum intercuspation of M1s, the contact areas increase both in number and extension mainly in the grooves and crests between the buccal cusps (between hypoconid and hypoconulid) showing how the first (grooves) canalize tensile stresses and the second (crests) locally biomechanically reinforce the crown (Benazzi et al., 2011).

In the case of the Croatian sample, the high values of enamel thickness identified in the functional cusps (Buccal area), as well as the buccal phase I extension together with dental shape of Bronze Age individuals (Fig. 4), could suggest a functional response of dental tissues to different mechanical loads.

In conclusion, the ETMP method provides the opportunity to evaluate the distribution of enamel thickness along dental crown. This will help to quantitatively compare enamel tissue strictly linked to masticatory, paramasticatory activities as well as parafunctional stress induced by malocclusion among populations. In particular from a biological perspective, the functional significance of enamel thickness along molar crowns will need to be considered for comparisons between humans and other primate species as a functional adaptation of a specific cultural and natural context. In a medical perspective, the thicker enamel on the cusp-lateral surfaces of the "functional" cusps (as a means to prolong functional crown life by preventing cusp fracture) should be considered during dental prosthesis preparation in order to find the best distribution of occlusal forces deriving from dental antagonists contact.

Declaration of competing interest

The authors declare that they have no known competing financial interests or personal relationships that could have appeared to influence the work reported in this paper.

Acknowledgment

The research was supported by the Croatian Science Foundation (Project: HRZZ IP-2016-06-1450 to M. N.).

Appendix A. Supplementary data

Supplementary data to this article can be found online at https://doi.org/10.1016/j.jas.2023.105776.

References

Adams, D.C., Otárola-Castillo, E., 2013. geomorph: an r package for the collection and analysis of geometric morphometric shape data. Methods Ecol. Evol. 4, 393–399. https://doi.org/10.1111/2041-210X.12035.

Anderson, M.J., 2001. A new method for non-parametric multivariate analysis of variance. Austral Ecol. 26, 32–46. https://doi.org/10.1111/j.1442-9993.2001.01070.

Balen, J., 2008. Apsolutni datumi sa zaštitnih istraživanja na prostoru Slavonije kao prilog poznavanju kronologije srednjeg eneolitika. Vjesnik Arheološkog muzeja u Zagrebu 41, 17–35.

Bayle, P., et al., 2010. Dental maturational sequence and dental tissue proportions in the early Upper Paleolithic child from Abrigo do Lagar Velho, Portugal. Proc. Natl. Acad. Sci. USA 107, 1338–1342. https://doi.org/10.1073/pnas.0914202107.

Been, E., et al., 2017. The first Neanderthal remains from an open-air Middle Palaeolithic site in the Levant. Sci. Rep. 7, 2958. https://doi.org/10.1038/s41598-017-03025-z.

Benazzi, S., et al., 2011. Using occlusal wear information and finite element analysis to investigate stress distributions in human molars. J. Anat. 219, 259–272. https://doi.org/10.1111/j.1469-7580.2011.01396.x.

Benazzi, S., et al., 2012. Cervical and crown outline analysis of worn Neanderthal and modern human lower second deciduous molars. Am. J. Phys. Anthropol. 149, 537–546.

Benazzi, S., et al., 2013a. Individual tooth macrowear pattern guides the reconstruction of Sts 52 (Australopithecus africanus) dental arches. Am. J. Phys. Anthropol. 150, 324–329.

Benazzi, S., et al., 2013b. Unravelling the functional biomechanics of dental features and tooth wear. PLoS One 8, e69990.

Benazzi, S., et al., 2013c. The evolutionary paradox of tooth wear: simply destruction or inevitable adaptation? PLoS One 8, e62263.

Benazzi, S., et al., 2014. Technical Note: guidelines for the digital computation of 2D and 3D enamel thickness in hominoid teeth. Am. J. Phys. Anthropol. 153, 305–313. https://doi.org/10.1002/ajpa.22421.
Benazzi, S., et al., 2015. Exploring the biomechanics of taurodontism. J. Anat. 226, 180–188. https://doi.org/10.1111/joa.12260.
Benazzi, S., et al., 2016. Dynamic modelling of tooth deformation using occlusal kinematics and finite element analysis. PLoS One 11 (3), e0152663. https://doi.org/10.1371/journal.pone.0152663.
Boljunčić, J., 1991. Anomalije na gornjim ljuskama zatiljnih kostiju dviju brončanodobnih čovječjih lubanja iz špilje Bezdanjače kod Vrhovina u Lici. Rad. Hrvat. Akad. Znan. Umjet. 458, 131–142.
Boljunčić, J., 1997. Analiza zatiljne kosti populacije ljudi iz bronča- nodobne nekropole u špilji Bezdanjači (Hrvatska). Prilozi Instituta za arheologiju u Zagrebu 11/12, 151–163.
Bortolini, E., et al., 2021. Early Alpine occupation backdates westward human migration in Late Glacial Europe. Curr. Biol. 31, 2484–2493.e7. https://doi.org/10.1016/j.cub.2021.03.078.
Carić, M., 2023. Diet and General Health of the Bronze Age Inhabitants of the Eastern Adriatic Coast and its Hinterland – Bioarchaeological and Biochemical Approach. Unpublished PhD thesis, University of Zagreb.
Carić, M., et al., 2020. Something old, something new: (re)analysis and interpretation of three Bronze Age trepanations from Croatia. Anthropologie 58, 39–51. https://doi.org/10.26720/anthro.19.12.06.1.
Carter, K., et al., 2014. News and views: non-metric dental traits and hominin phylogeny. J. Hum. Evol. 69, 123–128. https://doi.org/10.1016/j.jhevol.2014.01.003.
Dejak, B., et al., 2003. Finite element analysis of stresses in molars during clenching and mastication. J. Prosthet. Dent 90, 591–597. https://doi.org/10.1016/j.prosdent.2003.08.009.
Drechsler-Bižić, R., 1979. Nekropola brončanog doba u peći ni Bezdanjači kod Vrhovina. Vjesnik Arheološkog muzeja u Zagrebu 12/13, 27–32.
Dryden, I.L., et al., 1998. Statistical Shape Analysis 6.
Dumont, E.R., 1995. Enamel thickness and dietary adaptations among extant primates and chiropterans. J. Mammal. 76, 1127–1136.
Ebrahimi, M., et al., 2010. Dental treatment needs of permanent first molars in Mashhad schoolchildren. J. Dent. Res. 4, 52–55.
El Zaatari, S., et al., 2011. Ecogeographic variation in Neandertal dietary habits: evidence from occlusal molar microwear texture analysis. J. Hum. Evol. 61, 411–424. https://doi.org/10.1016/j.jhevol.2011.05.004.
Fiorenza, L., 2015. Reconstructing diet and behaviour of Neanderthals from Central Italy through dental macrowear analysis. J. Anthropol. Sci. 93, 119–133. https://doi.org/10.4436/JASS.93002, 2015.
Fiorenza, L., Kullmer, O., 2013. Dental wear and cultural behavior in middle paleolithic humans from the near east. Am. J. Phys. Anthropol. 152, 107–117. https://doi.org/10.1002/ajpa.22335.
Fiorenza, L., et al., 2011. Molar macrowear reveals Neanderthal eco-geographic dietary variation. PLoS One 6, e14769.
Fiorenza, L., et al., 2018. Functional relationship between dental macrowear and diet in Late Pleistocene and recent modern human populations. Int. J. Osteoarchaeol. 28, 153–161. https://doi.org/10.1002/oa.2642.
Fornai, C., et al., 2014. Enamel thickness variation of deciduous first and second upper molars in modern humans and Neanderthals. J. Hum. Evol. 76, 83–91. https://doi.org/10.1016/j.jhevol.2014.05.013.
Freilich, S., et al., 2021. Reconstructing genetic histories and social organisation in Neolithic and Bronze Age Croatia. Sci. Rep. 11, 16729 https://doi.org/10.1038/s41598-021-94932-9.
Gantt, D., et al., 2001. In: Distribution of Enamel Thickness on Human Deciduous Molars Brook. Dental Morphology. Sheffield Academic Press, pp. 167–190.
González-Rabanal, B., et al., 2022. The arrival of millets to the Atlantic coast of northern Iberia. Sci. Rep. 12 (1), 18589.
Grine, F.E., 1991. Computed tomography and the measurement of enamel thickness in extant hominoids: implications for its palaeontological application. Palaeont. afr. 28, 61–69.
Grine, F.E., 2002. Scaling of tooth enamel thickness, and molar crown size reduction in modern humans. South Afr. J. Sci. 98, 503–509.
Grine, F.E., 2005. Enamel thickness of deciduous and permanent molars in modern Homo sapiens. Am. J. Phys. Anthropol. 126, 14–31. https://doi.org/10.1002/ajpa.10277.
Grine, F.E., et al., 2001. Evaluation of dental radiograph accuracy in the measurement of enamel thickness. Arch. Oral Biol. 46, 1117–1125.
Grine, F.E., et al., 2004. Geographic variation in human tooth enamel thickness does not support Neandertal involvement in the ancestry of modern Europeans S. Afr. J. Sci. 100, 389–394.
Gunz, P., Mitteroecker, P., 2013. Semilandmarks: a method for quantifying curves and surfaces. Hystrix 24, 103–109.
Gunz, P., et al., 2005. Semilandmarks in three dimensions. In: Slice, D.E. (Ed.), Modern Morphometrics in Physical Anthropology, Developments in Primatology: Progress and Prospects. Kluwer Academic Publishers-Plenum Publishers, New York, pp. 73–98. https://doi.org/10.1007/0-387-27614-9_3.
Hasseldine, B.P.J., et al., 2017. Mechanical response of common millet (Panicum miliaceum) seeds under quasi-static compression: experiments and modeling. J. Mech. Behav. Biomed. 73, 102–113. https://doi.org/10.1016/j.jmbbm.2017.01.008.
Hiemae, K., Kay, R.F., 1972. Trends in the evolution of primate mastication. Nature 240, 486–487. https://doi.org/10.1038/240486a0.
Hinton, R.J., 1982. Differences in interproximal and occlusal tooth wear among prehistoric Tennessee Indians: implications for masticatory function. Am. J. Phys. Anthropol. 57, 103–115. https://doi.org/10.1002/ajpa.1330570111.
Hlusko, L.J., et al., 2004. Genetics and the evolution of primate enamel thickness: a baboon model. Am. J. Phys. Anthropol. 124, 223–233. https://doi.org/10.1002/ajpa.10353.
Horvath, J.E., et al., 2014. Genetic comparisons yield insight into the evolution of enamel thickness during human evolution. J. Hum. Evol. 73, 75–87. https://doi.org/10.1016/j.jhevol.2014.01.005.
Irish, J.D., et al., 2014. News and views: response to 'Non-metric dental traits and hominin phylogeny' by Carter et al., with additional information on the Arizona State University Dental Anthropology System and phylogenetic 'place' of Australopithecus sediba. J. Hum. Evol. 69, 129–134. https://doi.org/10.1016/j.jhevol.2014.01.004.
Janis, C.M., Fortelius, M., 1988. On the means whereby mammals achieve increased functional durability of their dentitions, with special reference to limiting factors. Biol. Rev. Camb. Phil. Soc. 63, 197–230. https://doi.org/10.1111/j.1469-185x.1988.tb00630.x.
Janković, I., Novak, M., 2021. The mysteries of the past – finds from the Bezdanjača Cave near Vrhovine. In: Janković, I., Drnić, I., Paar, D. (Eds.), Archaeology and Speleology: from the Darkness of the Underground to the Light of Knowledge. Archaeological Museum Zagreb, Zagreb, pp. 65–74.
Janković, I., et al., 2021. Mass violence in copper age Europe: the massacre burial site from Potočani, Croatia. Am. J. Phys. Anthropol. 176, 474–485. https://doi.org/10.1002/ajpa.24396.
Jovanović, J., et al., 2021. New radiocarbon dates, stable Isotope, and anthropological analysis of prehistoric human bones from the Balkans and Southwestern Carpathian Basin. Doc. Praehist. 48, 224–251. https://doi.org/10.4312/dp.48.18.
Kaidonis, J.A., et al., 1993. Nature and frequency of dental wear facets in an Australian aboriginal population. J. Oral Rehabil. 20, 333–340. https://doi.org/10.1111/j.1365-2842.1993.tb01615.x.
Kay, R.F., 1975. The functional adaptations of primate molar teeth. Am. J. Phys. Anthropol. 43, 195–216. https://doi.org/10.1002/ajpa.1330430207.
Kay, R.F., Hiiemae, K.M., 1974. Jaw movement and tooth use in recent and fossil primates. Am. J. Phys. Anthropol. 40, 227–256. https://doi.org/10.1002/ajpa.1330400210.
Khadijah, A., et al., 2020. Comparison of occlusal bite force distribution in subjects with different occlusal characteristics. Cranio. https://doi.org/10.1080/08869634.2020.1830662.
Kirleis, W., et al., 2022. Millet and what else? The Wider Context of the Adoption of Millet Cultivation in Europe 14 (Sidestone Press).
Kono, R.T., 2004. Molar enamel thickness and distribution patterns in extant great apes and humans: new insights based on a 3-dimensional whole crown perspective. Arch. Sci. 112, 121–146. https://doi.org/10.1537/ase.03106.
Kono, R.T., Suwa, G., 2008. Enamel distribution patterns of extant human and hominoid molars: occlusal versus lateral enamel thickness. Bull. Natl. Mus. Nat. Sci. D 34, 1–9.
Kono, R.T., et al., 2002. A three-dimensional analysis of enamel distribution patterns in human permanent first molars. Arch. Oral Biol. 47, 867–875. https://doi.org/10.1016/S0003-9969(02)00151-6.
Koolstra, J.H., et al., 1988. A three-dimensional mathematical model of the human masticatory system predicting maximum bite forces. J. Biomech. 21, 563–576.
Kullmer, O., et al., 2009. Technical note: occlusal fingerprint analysis: quantification of tooth wear pattern. Am. J. Phys. Anthropol. 139, 600–605. https://doi.org/10.1002/ajpa.21086.
Kullmer, O., et al., 2013. Dental arch restoration using tooth macrowear patterns with application to Rudapithecus hungaricus, from the late Miocene of Rudabánya, Hungary. J. Hum. Evol. 64, 151–160. https://doi.org/10.1016/j.jhevol.2012.10.009.
Lazaridis, I., et al., 2022. The genetic history of the southern arc: a bridge between west asia and Europe. Science 377, eabm4247. https://doi.org/10.1126/science.abm4247.
Le Luyer, M., et al., 2014. Brief communication: comparative patterns of enamel thickness topography and oblique molar wear in two Early Neolithic and medieval population samples. Am. J. Phys. Anthropol. 155, 162–172. https://doi.org/10.1002/ajpa.22562.
Los, Dž, 2020. Results of the archaeological excavations of the site an 2 Beli Manastir - Popova zemlja. Ann. Inst. Archaeol. 16, 90–102.
Lucas, P.W., et al., 2014. The role of dust, grit and phytoliths in tooth wear. Ann. Zool. Fenn. 51, 143–152. https://doi.org/10.5735/086.051.0215.
Macho, G.A., Berner, M.E., 1993. Enamel thickness of human maxillary molars reconsidered. Am. J. Phys. Anthropol. 92, 189–200.
Macho, G.A., Berner, M.E., 1994. Enamel thickness and the helicoidal occlusal plane. Am. J. Phys. Anthropol. 94, 327–337.
Macho, G.A., Spears, I.R., 1999. Effects of loading on the biochemical behavior of molars of Homo, Pan, and Pongo. Am. J. Phys. Anthropol. 109, 211–227.
Mahoney, P., 2010. Two-dimensional patterns of human enamel thickness on deciduous (dm1, dm2) and permanent first (M1) mandibular molars. Arch. Oral Biol. 55, 115–126. https://doi.org/10.1016/j.archoralbio.2009.11.014.
Maier, W., Schneck, G., 1981. Konstruktionsmorphologische Untersuchungen am Gebiß der hominoiden Primaten. Z. Morphol. Anthropol. 72, 127–169.
Malez, M., 1967. Kvartarološka i speleološka istraživanja u 1965. godini. Ljetopis Jugoslavenske akademije znanosti i umjetnosti 72, 405–417.
Malez, M., 1973. Prvi ljudi na teritoriju like. In: Gušić, B. (Ed.), Lika U Prošlosti I Sadašnjosti. Historijski Arhiv u Karlovcu, Karlovac, pp. 121–130.
Malez, M., 1979. Pećina Bezdanjača kod Vrhovina i njezina kvartarna fauna. Vjesnik Arheološkog muzeja u Zagrebu 12/13, 1–26.

Malez, M., Nikolić, V., 1975. Patološka pojava na čovječjoj lubanji iz pećine Bezdanjače u Lici. Rad. Jugosl. Akad. Znan. Umjet. 371, 171–179.
Malinar, H., 1976. Bezdanjača pod vatinovcem ili horvatova špilja. Naše planine 2, 21–25.
Mansour, R.M., Reynick, R.J., 1975. In vivo occlusal forces and moments, I: forces measured in terminal hinge position and associated moments. J. Dent. Res. 54, 114–120.
Margherita, C., et al., 2016. A reassessment of the presumed Torrener Bärenhöhle's Paleolithic human tooth. J. Hum. Evol. 93, 120–125. https://doi.org/10.1016/j.jhevol.2016.01.007.
Margherita, C., et al., 2017. Morphological description and morphometric analyses of the Upper Palaeolithic human remains from Dzudzuana and Satsurblia caves, western Georgia. J. Hum. Evol. 113, 83–90. https://doi.org/10.1016/j.jhevol.2017.07.011.
Martin, L., 1985. Significance of enamel thickness in hominoid evolution. Nature 314, 260–263. https://doi.org/10.1038/314260a0.
Martín-Francés, L., et al., 2020. Crown tissue proportions and enamel thickness distribution in the Middle Pleistocene hominin molars from Sima de los Huesos (SH) population (Atapuerca, Spain). PLoS One 15 (6), e0233281. https://doi.org/10.1371/journal.pone.0233281.
Martinoia, V., et al., 2021. Reconstructing the childhood diet of the individuals from the Middle Late Bronze Age Bezdanjača Cave, Croatia (ca. 1430 1290 BCE) using stable C and N isotope analysis of dentin collagen. J. bioanthropol. (Online) 1, 42–56. https://doi.org/10.54062/jb.1.1.3.
McClure, S.B., et al., 2020. Paleodiet and health in a mass burial population: the stable carbon and nitrogen isotopes from Potočani, a 6,200-year-old massacre site in Croatia. Int. J. Osteoarchaeol. 30, 507–518. https://doi.org/10.1002/oa.2878.
Mitteroecker, P., Gunz, P., 2009. Advances in geometric morphometrics. Evol. Biol. 36, 235–247. https://doi.org/10.1007/s11692-009-9055-x.
Molnar, S., 1971. Human tooth wear, tooth function and cultural variability. Am. J. Phys. Anthropol. 34, 175–189. https://doi.org/10.1002/ajpa.1330340204.
Molnar, S., Gantt, D.G., 1977. Functional implications of primate enamel thickness. Am. J. Phys. Anthropol. 46, 447–454. https://doi.org/10.1002/ajpa.1330460310.
Molnar, S., et al., 1993. Hominid enamel thickness. I. The krapina Neandertals. Am. J. Phys. Anthropol. 92, 131–138.
Novak, M., 2017. Bioarchaeological analysis of human bone remains from site Beli Manastir - Popova zemlja (AN2). Unpublished Expert Report BA1-05/17. Institute for Anthropological Research, Zagreb.
Novak, M., et al., 2021. Genome-wide analysis of nearly all the victims of a 6200 year old massacre. PLoS One 16, e0247332. https://doi.org/10.1371/journal.pone.0247332.
Olejniczak, A.J., Grine, F.E., 2006. Assessment of the accuracy of dental enamel thickness measurements using microfocal X-ray computed tomography. Anat. Rec. A Discov. Mol. Cell. Evol. Biol. 288, 263–275. https://doi.org/10.1002/ar.a.20307.
Olejniczak, A.J., et al., 2008a. Dental tissue proportions and enamel thickness in Neandertal and modern human molars. J. Hum. Evol. 55, 12–23.
Olejniczak, A.J., et al., 2008b. Three-dimensional molar enamel distribution and thickness in Australopithecus and Paranthropus. Biol. Lett. 4, 406–410.
Olejniczak, A.J., et al., 2008c. Three-dimensional primate molar enamel thickness. J. Hum. Evol. 54, 187–195. https://doi.org/10.1016/j.jhevol.2007.09.014.
Oxilia, G., et al., 2015. Earliest evidence of dental caries manipulation in the Late Upper Palaeolithic. Sci. Rep. 5, 12150 https://doi.org/10.1038/srep12150.
Oxilia, G., et al., 2017. The dawn of dentistry in the late upper Paleolithic: an early case of pathological intervention at Riparo Fredian. Am. J. Phys. Anthropol. 163, 446–461. https://doi.org/10.1002/ajpa.23216.
Oxilia, G., et al., 2018. The physiological linkage between molar inclination and dental macrowear pattern. Am. J. Phys. Anthropol. 166, 941–951. https://doi.org/10.1002/ajpa.23476.
Oxilia, G., et al., 2021a. Exploring late Paleolithic and Mesolithic diet in the Eastern Alpine region of Italy through multiple proxies. Am. J. Phys. Anthropol. 174, 232–253. https://doi.org/10.1002/ajpa.24128.
Oxilia, G., et al., 2021b. Exploring directional and fluctuating asymmetry in the human palate during growth. Am. J. Phys. Anthropol. 175, 847–864. https://doi.org/10.1002/ajpa.24293.
Oxilia, G., et al., 2022. Direct evidence that late Neanderthal occupation precedes a technological shift in southwestern Italy. Am. J. Phys. Anthropol. 179, 18–30. https://doi.org/10.1002/ajpa.24593.
Pampush, J.D., et al., 2013. Homoplasy and thick enamel in primates. J. Hum. Evol. 64, 216–224. https://doi.org/10.1016/j.jhevol.2013.01.009.
Paul, K.S., Stojanowski, C.M., 2015. Performance analysis of deciduous morphology for detecting biological siblings. Am. J. Phys. Anthropol. 157, 615–629. https://doi.org/10.1002/ajpa.22755.
Pavičić, T., 2015. Jagodnjak – krčevine – selska bara (AN 7). Hrvatski arheološki godišnjak 12, 39–41.
Pechenkina, E.A., et al., 2002. Diet and health changes at the end of the Chinese neolithic: the Yangshao/Longshan transition in Shaanxi province. Am. J. Phys. Anthropol. 117, 15–36. https://doi.org/10.1002/ajpa.10014.
Percač, S., 1992. Morphological characteristics of human lower jaws of the Eneolithic population of the Bezdanjača cave (Croatia). Rad. Hrvat. Akad. Znan. Umjet. 463, 81–90.
Potrebica, H., Balen, J., 2008. Rekognosciranje južnih obronaka papuka (zona velika - stražeman). Hrvatski arheološki godišnjak 4, 116–119.
Pruim, G.J., et al., 1980. Forces acting on the mandible during bilateral static bite at different bite force levels. J. Biomech. 13, 755–763.
R Core Team, R.C., 2021. R: A Language and Environment for Statistical Computing. R Foundation for Statistical Computing, Vienna, Austria. http://www.R-project.org/.
Rohlf, F.J., Slice, D., 1990. Extensions of the Procrustes method for the optimal superimposition of landmarks. Syst. Biol. 39, 40–59. https://doi.org/10.2307/2992207.
Romandini, M., et al., 2020. A late Neanderthal tooth from northeastern Italy. J. Hum. Evol. 147, 102867 https://doi.org/10.1016/j.jhevol.2020.102867.
Rozzi, F.R., 1996. Comment on the causes of thin enamel in Neandertals. Am. J. Phys. Anthropol. 99, 625–626.
Saadi, A.S.A., et al., 2023. 2D and 3D wear analysis of 3D printed and prefabricated artificial teeth. Int. Dent. J. 73, 87–92. https://doi.org/10.1016/j.identj.2022.10.002.
Sathyanarayana, H.P., et al., 2012. Assessment of maximum voluntary bite force in adults with normal occlusion and different types of malocclusions. J. Contemp. Dent. Pract. 13, 534–538.
Schwartz, G.T., 2000a. Taxonomic and functional aspects of the patterning of enamel thickness distribution in extant large-bodied hominoids. Am. J. Phys. Anthropol. 111, 221–244.
Schwartz, G.T., 2000b. Enamel thickness and the helicoidal wear plane in modern human mandibular molars. Arch. Oral Biol. 45, 401–409.
Shellis, R.P., 1998. Utilization of periodic markings in enamel to obtain information on tooth growth. J. Hum. Evol. 35, 387–400. https://doi.org/10.1006/jhev.1998.0260.
Shillingburg, H.T., Grace, C.S., 1973. Thickness of enamel and dentin South. Calif. State Dent. Assoc. 41, 33–52.
Skinner, M., 2008. Enamel-dentine Junction Morphology of Extant Hominoid and Fossil Hominin Lower Molars. The George Washington University.
Skinner, M.M., et al., 2015. Enamel thickness trends in Plio-Pleistocene hominin mandibular molars. J. Hum. Evol. 85, 35–45. https://doi.org/10.1016/j.jhevol.2015.03.012.
Šlaus, M., 2002. The Bioarchaeology of Continental Croatia. An Analysis of Human Skeletal Remains from the Prehistoric to Post-medieval Periods. Archaeopress, Oxford.
Slice, D.E., 2006. Modern Morphometrics in Physical Anthropology. Springer Science & Business Media.
Smith, B.H., 1984. Patterns of molar wear in hunger-gatherers and agriculturalists. Am. J. Phys. Anthropol. 63, 39–56. https://doi.org/10.1002/ajpa.1330630107.
Smith, P., Zilberman, U., 1994. Thin enamel and other tooth components in Neanderthals and other hominids. Am. J. Phys. Anthropol. 95, 85–87.
Smith, T.M., et al., 2005. Variation in hominoid molar enamel thickness. J. Hum. Evol. 48, 575–592. https://doi.org/10.1016/j.jhevol.2005.02.004.
Smith, T.M., et al., 2006. Modern human molar enamel thickness and enamel-dentine junction shape. Arch. Oral Biol. 51, 974–995. https://doi.org/10.1016/j.archoralbio.2006.04.012.
Smith, T.M., et al., 2008. Brief communication: enamel thickness trends in the dental arcade of humans and chimpanzees. Am. J. Phys. Anthropol. 136, 237–241.
Smith, T.M., et al., 2009. Tafforeau Taxonomic Assessment of the Trinil Molars Using Non-destructive 3D Structural and Developmental Analysis PaleoAnthropol 117-129.
Smith, T.M., et al., 2012. Variation in enamel thickness within the genus Homo. J. Hum. Evol. 62, 395–411. https://doi.org/10.1016/j.jhevol.2011.12.004.
Sonnesen, L., Bakke, M., 2005. Molar bite force in relation to occlusion, craniofacial dimensions, and head posture in pre-orthodontic children. Eur. J. Orthod. 27, 58–63.
Sorrentino, R., et al., 2018. Unravelling biocultural population structure in 4th/3rd century BC Monterenzio Vecchio (Bologna, Italy) through a comparative analysis of strontium isotopes, non-metric dental evidence, and funerary practices. PLoS One 13 (3), e0193796.
Spears, I.R., Macho, G.A., 1995. The Helicoidal Occlusal Plane—A Functional and Biomechanical Appraisal of Molars Proceedings of the 10th International Symposium on Dental Morphology. M" Marketing Services, Berlin.
Spencer, M.A., 1995. Masticatory System Configuration and Diet in Anthropoid Primates. Ph.D. dissertation, State University of New York at Stonybrook.
Spencer, M.A., 1998. Force production in the primate masticatory system: electromyographic tests of biomechanical hypotheses. J. Hum. Evol. 34, 25–54.
Spoor, C.F., et al., 1993. Linear measurements of cortical bone and dental enamel by computed tomography: applications and problems. Am. J. Phys. Anthropol. 91, 469–484.
Stober, T., et al., 2006. Wear of resin denture teeth by two-body contact. Dent. Mater. 22, 243–249.
Suwa, G., et al., 2009. Paleobiological implications of the Ardipithecus ramidus dentition. Science 326, 70–99.
Traversari, M., et al., 2019. Multi-analytic study of a probable case of fibrous dysplasia (FD) from certosa monumental cemetery (Bologna, Italy). Int. J. Paleopathol. 25, 1–8. https://doi.org/10.1016/j.ijpp.2019.03.003.
Tuniz, C., et al., 2013. The ICTP-Elettra X-ray laboratory for cultural heritage and archaeology. Nucl. Instrum. Methods Phys. Res.: Accel. Spectrom. Detect. Assoc. Equip. 711, 106–110. https://doi.org/10.1016/j.nima.2013.01.046.
Vandkilde, H., et al., 2015. Cultural mobility in Bronze age Europe. Introduction. In: Suchowska-Ducke, Paulina, Scott Reiter, Samantha, Vandkilde, Helle (Eds.), Mobility of Culture in Bronze Age Europe. (British Archaeological Reports, S2771. Archaeopress, Oxford, GB.
Varalli, A., et al., 2022. A multi-proxy bioarchaeological approach reveals new trends in Bronze Age diet in Italy. Sci. Rep. 12, 12203 https://doi.org/10.1038/s41598-022-15581-0.
Vazzana, A., et al., 2018. A multianalytic investigation of weapon-related injuries in a Late Antiquity necropolis. Mutina, Italy. J. Archaeol. Sci. Rep. 17, 550–559.

Zanolli, C., 2015. Molar crown inner structural organization in Javanese Homo erectus. Am. J. Phys. Anthropol. 156, 148–157.

Zavodny, E., et al., 2017. Minimizing risk on the margins: insights on Iron Age agriculture from stable isotope analyses in central Croatia. J. Anthropol. Archaeol. 48, 250–261. https://doi.org/10.1016/j.jaa.2017.08.004.

Zilberman, U., et al., 1992. Tooth components of mandibular deciduous molars of *Homo sapiens sapiens* and *Homo sapiens neanderthalensis*: a radiographic study. Am. J. Phys. Anthropol. 87, 255–262.